Jurnal Mekanikal
Jun 2004, Bil. 17, 56 - 86

MODELLIZATION OF THE SPECIAL SEGMENTED RUBBER TRACKED VEHICLE DESIGN PROCESSES ON PEAT TERRAIN IN MALAYSIA

[1]Ataur Rahman
Azmi Yahaya
Mohd. Zohadie Bardaie
Desa Ahmad
Wan Ishak Bin Wan Ismail

Faculty of Engineering
Universiti Putra Malaysia
43400 UPM, Serdang
Selangor D.E, Malaysia

ABSTRACT

Discussion on the modellization of an off-road special segmented rubber tracked vehicle on low bearing capacity Sepang peat terrain design processes is the main focus of this paper. To complete this study, first the mechanical properties of peat terrain were determined by using different type of apparatus. Direct shear test was performed using a Wykeham Farrance 25402 shear box apparatus to determine the internal friction angle, cohesiveness and shear deformation modulus of the peat sample. Load-sinkage test was performed using a specially made bearing capacity apparatus to determine the stiffness values of surface mat and underlying peat. Secondly, mathematical model was developed for computing the vehicle tractive performance. Thirdly, design parameters of the special segmented rubber tracked vehicle were optimized by simulation method using Microsoft Excel with analyzing the information and managing list in powerful spreadsheet. Finally, vehicle design was completed based on the simulated optimized design parameters by using Auto-CAD software package.

***Keywords**: Tracked vehicle, Peat terrain, bearing capacity, Tractive performance.*

1.0 INTRODUCTION

New requirements for greater mobility over a wide range of peat terrain, and growing demands for environmental protection and collection-transportation goods by vehicles on unprepared peat terrain constitute a significant part of the overall transportation activities. This has led to the necessity of developing segmented rubber tracked vehicle and establishing mathematical models for the vehicle-peat terrain systems, that will enable design engineers, to evaluate a wide range of options for the selection of an optimum configuration for a given mission and environment. There are different organizations in Malaysia that

[1] Corresponding Author : Ataur Rahman, E-mail: Ataur979@yahoo.com

introduced different type of machines for infield collection-transportation operations on peat land. All of the machines suitability was justified based on the mechanical properties of Sepang peat land. It was found that the engine power of all the machines is quite reasonable based on their load carrying capacity. But, tractive performance is severely effect due to their higher ground pressure distribution. For example, Super Crawler [1], it was found that the machine is not suitable to traverse on Sepang peat terrain due to its higher shearing-off the surface mat and ground pressure distribution of 15.44% is higher than the bearing capacity of the Sepang peat terrain in Malaysia, which might severely affect the vehicle sinkage. For Peat Prototype Tracked Tractor [2] and FFB Ficker MRK-1 [3], it was found that none of these machine is suitable to traverse on peat terrain due their ground pressure distribution of 12%, 15.4% and 79%, respectively higher than the bearing capacity of the worst condition peat terrain of Malaysia. The other problems were found for the FFB Ficker MRK-1 that these machines track used to slip out from the wheel during turning. For Kubota KC-50 [4] Hitachi EG30- Rubber Crawler Carrier [5] and SEIREI-SC3.SC3W Rubber Crawler Carrier [6] was found that none of these machine is suitable to traverse on worst condition Sepang peat terrain in Malaysia due to their ground pressure distribution of 32.7%, 96%, 44%, and 38.5%, respectively higher than the bearing capacity of worst condition Sepang peat terrain.

It is urgent to develop a new machinery system operating on peat terrain to lower the maintenance cost. The disadvantage here is that the bearing capacity of Malaysian tropical peat terrain is 17kN/m^2. Consequently, it is considered to be very difficult to develop any working vehicle that could run and operate on the low trafficability peat terrain. As a first step in the design of vehicles for work over peat terrain, it is necessary to establish the technical feasibility of tracked vehicles having large contact area and low ground contact pressure suitable for weak terrain in comparison to a wheeled vehicle. Hence, a research and development program to produce a new vehicle system for peat terrain is proposed to solve the problem. Such vehicle has a potentially very large market in Malaysia to be used for infield collection-transportation oil palm on peat terrain.

This paper describes the development of a new machine system through understanding of tracked-terrain interaction process. The effect of a number of subtle factors: tracked size, idler and sprocket size and geometric location, number of road-wheels and geometric arrangement and position of the center of gravity of the vehicle, which influence the vehicle tractive performance during running in straight-line motion was studied. In this paper, the method for determining the mechanical properties of peat and a mathematical model for determining the vehicle tractive performance is developed. Based on a given set of vehicle dimensions and terrain-track system constants, a simulation technique is then used to optimize the design parameters of the vehicle by the calculation of tractive effort, amount of sinkage and slippage of the tracked ground contact part

of tracked main straight part, front idler and rear sprocket and tracked entry and exit angle.

2.0 MATERIALS AND METHODS

The feasibility of the land locomotion of the tracked vehicle operating on the weak peat terrain is discussed from the perspective of the field of terramechanics. For example, the mobility of a tracked vehicle having an average ground contact pressure of 15 to 50kN/m^2 was investigated using terramechanical simulation analysis. Figure 1 shows the processes of designing a segmented tracked vehicle.

2.1 Mechanical Properties of Peat Terrain

The key to the segmented tracked vehicle performance prediction lies in the proper evaluation of the mechanical properties of the terrain. A ground vehicle applies horizontal load to the peat terrain through its running gear and this results in the development of thrust and an associated slip. The vertical load that a vehicle exerts on the terrain results in sinking giving rise to motion resistance. The measurement of both horizontal and vertical load-deformation characteristics of peat are of prime importance in the evaluation of the vehicle performance. To properly identify the mechanical properties of peat from a vehicle mobility viewpoint, measurement has been taken under loading conditions similar to those exerted by a vehicle on the peat terrain. Field tests were carried out at Sepang peat area, to determine the mechanical properties of peat terrain including moisture content, bulk density, cohesiveness, internal friction angle, shear deformation modulus, vane shearing strength, surface mat stiffness, and underlying stiffness of peat.

The area was heavily infested with palm roots, low shrubs, grasses, and sedges. The field conditions were wet and the water table was found to be 0 to 12 cm below the surface level. The surface mat and the peat deposit thickness were not distinct by visual observation. The surface mat thickness was about 5 to 25 cm at the center location between adjacent palm rows and 10 to 35 cm at the palm tree location. The underlying peat deposit thickness for the whole area was about 50 to 100 cm. The water field capacity was almost at saturation level and walking on such a terrain condition was only possible with the use of a special made wooden clog. The dominant features of this site may be described as high water content and weak underlying peat that could easily be disturbed by vehicle movements. The overall area was divided into 3 equal area blocks and each block was again divided into 3 equal sub-blocks. *In-situ* determinations for vane shearing strength, surface mat stiffness, and underlying stiffness were carried out at 10cm, 25cm and 40cm depth in triplet replications at the center location between adjacent palm rows within each sub-block in the field during un-drained and drained conditions. Similarly, undisturbed sample of 216 cm^3 volume were taken at the mentioned depths and points in the fields in triplet replications for the

determinations of moisture content, bulk density, cohesiveness, internal friction angle, shear deformation modulus of peat. The samples were wrapped with aluminum foil paper and sealed in a plastic container before they were immediately taken to the laboratory for the relevant analysis.

2.1.1 Moisture Content and Bulk Density

The collected samples that were brought to the laboratory were initially weighted for their wet mass before placing in an electric oven at 105°C temperature. After twenty-four hours, the samples were taken out from the oven and weighted for their dry mass. The sample moisture content is defined as the percentage ratio between the differences in sample wet mass and dry mass in gram with the sample wet mass in gram. The sample bulk density was computed by dividing the sample dry mass in gm to the sample known volume in cm^3.

2.1.2 Cohesiveness, Internal Friction Angle, and Shear Deformation Modulus

A Wykeham Farrance 25402 shear box apparatus shown in Figure 2 was used to determine cohesiveness, internal friction angle, and bulk deformation modulus of peat. The apparatus was setup to run at a shear rate of 0.25 mm/sec and a maximum shear displacement of 12mm.

Prior to the actual shear test, the prepared test sample in the rectangular box was subjected to a consolidation load of 1 kg for 24 hours. Readings on the shear displacement in cm and shearing strength in kN/m^2 was recorded for every minute until failure on the sample. The same test procedure was repeated for the consolidation load of 1.5kg and 2 kg, and again repeated on samples taken from different depths, different sampling points, and different drainage conditions.

For the shear deformation modulus of peat, the relationship between the shear deformation modulus K, the maximum shearing stress τ_{max} and τ and the corresponding shear displacement j , can be modeled by using the model equation of Wong et. al. [7]:

$$K = -\frac{\sum\left(1-\frac{\tau}{\tau_{max}}\right)^2 j^2}{\sum\left(1-\frac{\tau}{\tau_{max}}\right)^2 j\left[\ln\left(1-\frac{\tau}{\tau_{max}}\right)\right]} \tag{1}$$

The typical trend of shearing stress versus shear displacement and the shearing stress versus normal stress for a sample are shown in Figure 3 and Figure 4 respectively. From the interpretation of normal stress and shearing stress, the cohesiveness and the internal friction angle of peat were computed. Information of shear deformation modulus, cohesion, and internal friction angle could be used in the computations of traction, engine power, drawbar power, and tractive efficiency of a vehicle.

2.1.3 In-situ Shearing Stress

A RMU I012 digital vane test apparatus shown in Figure 5 was used to determine the *in-situ* shearing stress of peat. The apparatus comprises of a set of hollow rods for holding the vane blade, a twisting instrument on the upper end for twisting the rod set, and a digital measuring gearbox for measuring the twisting torque. The digital measuring gearbox is powered by 12voltage DC battery. Three vane blades having a diameter of 4.4cm, 5.4cm, and 6.4cm were used to shear the peat. This apparatus was setup to run at a twisting torque ranging from 500 to 600kg-cm at an accuracy of 1kg-cm resolution.

Prior to the actual test, the digital measuring gearbox was calibrated. During the operation of the apparatus for the shear test, the twisting instrument was rotated at a speed of 12deg/sec to shear the peat. Reading on the twisting torque was recorded for every 7.5 seconds until a complete 360° rotation. The maximum twisting torque of a complete 360^0 rotation was recorded. The measured value was later used to compute the shear stress of the peat. The same test procedure was repeated for different depths, different blades with diameter of 5.4cm and 6.4cm, different sampling points, and different drainage conditions.

For the shearing stress of the peat *in-situ*, the relationship between the shearing stress τ_f, torque of the rotating vane T, the radius of the vane r, and H height of the vane can be modeled by the following equation:

$$\tau_f = \frac{3T}{2\pi r^2 (2r+3H)} \qquad (2)$$

2.1.4 Surface Mat Stiffness and Underlying Stiffness of Peat

A specially developed apparatus as shown in Figure 6 was used to determine the surface mat stiffness and underlying stiffness of peat. The apparatus comprises of a proof ring with a dial gauge for measuring the force, a shaft with a diameter of 1.59 cm and length of 45 cm for transferring load to sinkage plate and a rectangular plate with a size of 15x5x0.5cm for measuring the sinkage. Three sinkage plates having a diameter of 10cm and 15cm and a size of 15x5cm were used to determine the stiffness of peat. This apparatus was setup to run at a proving ring constant of 0.2 kg / division.

Prior to the actual stiffness test, the proof ring dial gauge was calibrated. During the operation of the apparatus for the stiffness test, the long shaft with sinkage plate diameter of 10cm was manually pushed into the soil surface at an approximate speed of 2.5cm/sec. Reading on the pushing load in kg and sinkage in cm was recorded for every 2cm plate sinkage. The measured value was later used to plot a graph as shown in Figure 7. The parameter characterizing the behavior of the surface mat that is represented by '*m*' was determined from the slope of the Figure 7 regression line. The same test procedure was repeated for sinkage plates with diameters of 5.4cm and 6.4cm, different sampling points, and different drainage conditions.

For the surface mat stiffness and underlying stiffness of peat, the relationship between the normal load p, surface mat stiffness m_m, underlying stiffness of peat k_p, the size of the sinkage plate can be modeled by using the model equation of Wong [8]:

$$p = \frac{1}{100}\left[k_p z + mk_p z^2 (L/A)\right] \tag{3}$$

with $m_m = mk_p$

2.2 MATHEMATICAL FORMULATION

Considering a rigid link segmented rubber track vehicle of weight W, track size including track ground contact length L, width B, pitch T_p, and grouser height H, radius of the front idler R_{fi} , rear sprocket R_{rs}, and road-wheel R_w, and height of center of gravity (C.G) h_{cg}, is traversing under traction on a peat terrain at a constant speed of v_t as soon as applying driving torque Q at the rear sprocket by the hydraulic motor as shown in Figure 2. If the pressure distribution in the track-terrain interface is assumed to be non-uniform by locating vehicle C.G at ahead of the track mid point, the vehicle will traverse on the specified terrain by making an angle θ_{ti}. Consequently, the track entry and exit angle at the front idler θ_{fi} and rear sprocket θ_{rs}, the reaction pressure at the front idler P_{fi}, main straight part P_o, and rear sprocket P_{rs}, and the sinkage of the front idler z_{fi}, main straight part z_{mp}, and rear sprocket z_{rs} and tangential force will reveal different value due to the different amount of slippage at each of the grouser positions of the rigid link tracks at the bottom track elements of the front idler i_{fi}, main straight parts i_{mp} , and rear sprocket i_{rs} as shown in Figure 8.

The following assumptions are made in order the equation used in the mathematical modeling to be validated:

i. Vehicle theoritical speed is considered to be 10 km/hr on zero slop terrain based on various off-road operation ASAE D497.3 NOV96, ASAE standard [9]
ii. Vehicle total weight is considered to be 19.62 kN with payload of 9.81kN based on the in-field maximum fresh bounces collection practiced
iii. Vehicle's track critical sinkage is considered to be 0.1m based on experimental data on Sepang Peat terrain Ataur et.al. [10].
iv. Aerodynamic resistance has been neglected, due to the low operating speed
v. Vehicle's belly drag is considered to be zero since the vehicle hull is not in contact with the terrain
vi. Vehicle speed fluctuation is considered to be 2.75% based on Wong [9]
vii. Road-wheel spacing is considered to be 0.245m to ensure good drawbar performance based on Wong [9]

2.2.1 Tractive Effort

Tractive effort may be defined as the tractive force of the vehicle, which can be mobilized at the terrain interface. It is developed not only on the ground contact part of the vehicle track but also on the side parts of the grouser of the ground contact track. The traction mechanics of the track bottom part of the front idler, road-wheels, and the rear sprocket are different due to its different angle of entry and angle of exit. Therefore, it is important to compute the tractive effort of the vehicle undercarriage individual moving components bottom track segments such as front idler, track main straight part, and front idler, respectively.

(a) Ground Contact Part of the Track

The traction mechanics of the track bottom part of the front idler, road-wheels, and rear sprocket are different due to its different angle of entry and exit. It is also different due to the different sinkage of the track front idler, main straight part, and rear sprocket when the vehicle will traverse on the unprepared peat terrain with non-uniform ground pressure distribution. Therefore, it is important to compute the traction of the individual components bottom track segment, separately.

For the tractive effort developed at the track ground contact length, the relationship between the tractive effort F_b developed at the ground contact track, track ground contact length L, track width B, terrain cohesiveness c, normal stress σ, shear stress τ, shear deformation modulus K_w, slippage of the track-terrain interfaces i and shear displacement j_x can be modeled by the following equation of Bekker [11] given first in general formulation:

$$F_b = 2B\int_0^L \tau dx \tag{4}$$

with $\tau = \tau_{\max}\left(\frac{j_x}{K_w}\right)\exp\left(1-\frac{j_x}{K_w}\right)$ where, $\tau_{\max} = (c+\sigma\tan\varphi)$ and $j_x = ix$

By integrating the equation (1), the tractive effort of the vehicle can be computed as follows:

$$F_b = 2BL\,(c + \sigma\tan\varphi)\left[\frac{e^1 K_w}{iL} - \left(1+\frac{K_w}{iL}\right)\exp\left(1-\frac{iL}{K_w}\right)\right] \tag{5}$$

For the peat terrain and the slippage by equations (8), (9) and (10), the ground contact part of the front idler track elements as in Figure 9(a) is derived as,

$$F_{fib} = 2BL_{fib}\,(c + \sigma\tan\varphi)\left[\frac{e^1 K_{wfi}}{i_{fi} L_{fib}} - \left(1+\frac{K_{wfi}}{i_{fi} L_{fib}}\right)\exp\left(1-\frac{i_{fi} L_{fib}}{K_{wfi}}\right)\right] \tag{6}$$

with $L_{fib} = R_{fi}(\theta_{fi} + \theta_{ti})$

For the ground contact part of main straight track elements as in Figure 9(b):

$$F_{mb} = 2BL(c + \sigma \tan \varphi)\left[\frac{e^1 K_{wmb}}{i_{mb} L} - \left(1 + \frac{K_{wmb}}{i_{mb} L}\right)\exp\left(1 - \frac{i_{mb} L}{K_{wmb}}\right)\right] \quad (7)$$

with $i_{mb} = \dfrac{i_{fi} + i_{rs}}{2}$

For the ground contact part of the rear sprocket track elements as in Figure 9(c):

$$F_{rsb} = 2BL_{rsb}(c + \sigma \tan \varphi)\left[\frac{e^1 K_{wrs}}{i_{rs} L_{rsb}} - \left(1 + \frac{K_{w\,rs}}{i_{rs} L_{rsb}}\right)\exp\left(1 - \frac{i_{rs} L_{rsb}}{K_{wrs}}\right)\right] \quad (8)$$

with $L_{rsb} = R_{rs}\theta_{rs}$

(b) Side of the Ground Contact Track

The traction mechanics of the track at the side of the grouser is highly significant on the development of vehicle traction if the vehicle sinkage is more than the grouser height [12]. In this study, it is assumed that the sinkage of the vehicle is more than the grouser height of the track.

For the tractive effort developed at the side of the ground contact length of the track, the relationship between the tractive effort F_s developed at the side of the track ground contact part, track grouser height H, track ground contact length L, terrain cohesiveness c, normal stress σ, shear stress τ, shear deformation modulus K_w, and slippage i of the vehicle track-terrain interfaces can be modeled by the following equation of Wong [9] given first in general formulation:

$$F_s = 4H\cos\alpha \int_0^L \tau dx \quad (9)$$

with $\tau = \tau_{\max}\left(\dfrac{j_x}{K_w}\right)\exp\left(1 - \dfrac{j_x}{K_w}\right)$, $\tau_{\max} = (c + \sigma \tan \varphi)$ and $j_x = ix$

By integrating the equation (6), the tractive effort of the vehicle can be computed as follows:

$$F_s = 4HL(c + \sigma \tan \varphi)\cos\alpha\left[\frac{e^1 K_w}{iL} - \left(1 + \frac{K_w}{iL}\right)\exp\left(1 - \frac{iL}{K_w}\right)\right] \quad (10)$$

For the peat terrain, the side of the ground contact part of front idler track element is expressed as,

$$F_{fis} = 4HL_{fib}(c + \sigma \tan \varphi)\cos\alpha\left[\frac{e^1 K_{wfi}}{i_{fi} L_{fib}} - \left(1 + \frac{K_{wfi}}{i_{fi} L_{fib}}\right)\exp\left(1 - \frac{i_{fi} L_{fib}}{K_{wfi}}\right)\right] \quad (11)$$

with $\alpha = \arctan\left[\cot\left(\dfrac{H}{B}\right)\right]$

For the side of the ground contact part of main straight track element:

$$F_{ms} = 4HL(c + \sigma \tan\varphi)\cos\alpha\left[\frac{e^1 K_{wmb}}{i_{mp} L} - \left(1 + \frac{K_{wmb}}{i_{mp} L}\right)\exp\left(1 - \frac{i_{mp} L}{K_{wmb}}\right)\right] \quad (12)$$

For the side of the ground contact part of rear sprocket track element:

$$F_{rss} = 4HL_{rsb}(c + \sigma \tan\varphi)\cos\alpha\left[\frac{e^1 K_{wrs}}{i_{rs} L_{rsb}} - \left(1 + \frac{K_{wrs}}{i_{rs} L_{rsb}}\right)\exp\left(1 - \frac{i_{rs} L_{rsb}}{K_{wrs}}\right)\right] \quad (13)$$

The total thrust of the rubber track vehicle F_{tt}, can be computed as the sum of the individual thrust components by:

$$F_{tt} = F_{fib} + F_{mb} + F_{rsb} + F_{fis} + F_{ms} + F_{rss} \quad (14)$$

3.0 MATHEMATICAL MODEL VALIDATION

The drawbar pull and the tractive efficiency of light peat prototype Kubota Carrier RC20P track vehicle having track size of 0.43m width and 1.85m track ground contact length and total weight of 2645kg including payload 1000kg and three pneumatic road-wheels on each track, operating on a peat terrain were predicted through simulation method. Basic parameters of the reference vehicle that used in the study have shown in Table 1. The predicted performance was compared with filed test data provided by Malaysian Agricultural Research and Development Institute [13] as shown in Figures 10 and 11 in order to substantiate the validity of the new mathematical model.

Figure 10 shows that the predicted drawbar pull has an error of +15%, +15.8%, +18.27% and +2.68% on the measured drawbar pull for slippage of 5%, 10%, 20%, and 50% , respectively. Similarly Figure 11 shows that the predicted tractive efficiency has an error of +4.34%, +1.46%, +4.5%, and +28% on the measured tractive efficiency of the vehicle for slippage of 5%, 10%, 20%, and 50% , respectively. Therefore, the close agreement between the predicted and measured drawbar pull and tractive efficiency substantiates the validity of the simulation model.

4.0 DESIGN PARAMETERS SELECTION METHOD

Based on the developed new mathematical model for undrained peat terrain, it appeared that the engine size and tractive performance of the vehicle vary with the variation of vehicle weight, track size including track ground contact length,

width, pitch and grouser height, track entry and exit angle, idler diameter and location, sprocket diameter and location, road-wheel diameter, spacing and geometrical arrangement, and location of center of gravity. Therefore, for the selection and optimization design parameters of the vehicle most of these quantities to be taken into account.

4.1 Track Width and Ground Contact Length

To evaluate the effects of track system configuration on vehicle ground pressure distribution and surface mat stiffness, it is important to study track ground contact length and width. Figures 12(a) and 12(b) show that the vehicle ground pressure distribution decreases with increasing vehicle track ground contact length and width. The vehicles under consideration are traversing on a zero slope terrain at 9 % slippage and travel speed of 10km/hr. From the field experiment on Sepang, it was found that the bearing capacity for the undrained peat terrain was 17kN/m^2. It appears that if the ground contact pressure of the 19.62kN vehicle with a moderate payload of 9.81kN is limited to 16.35kN/m^2 by designing a track with ground contact area of 2.0X0.3m^2 then the sinkage and external motion resistance of the vehicle will be low and tractive effort will be high, yielding desired travel speed of 10km/h and vehicle productivity.

Figures 13 (a) and 13(b) show that the sinkage of the vehicle decreases with increasing track width and track ground contact length. If the track size of the vehicles is limited to 0.30x2.0m, then the sinkage of the 11.77kN, 17.65kN, and 21.52kN vehicles will be 6.1, 8.18, and 11cm, respectively. From the field experiment, it was found that the surface mat thickness of the Sepang peat terrain was 0.10m, which will support the maximum load of the vehicle during static and dynamic as well. Therefore, if the vehicle sinkage is more than 10cm the vehicle will sink rather than traverse. It could be pointed out that if the 19.62kN vehicle sinkage is limited to 0.1m it would be optimized the track ground contact area for the vehicle of 2.0X0.3m^2.

The conclusion is further supported by the relation between the track size and motion resistance. Figures 14(a) and 14(b) show that the motion resistance coefficient of the vehicle decreases with increasing track width and track ground contact length. From the figures, it was found that the motion resistance of the vehicle increased 18% with increasing the track width from 0.25 to 0.45m when the track ground contact length is kept constant at 2.0m. While, the motion resistance of the vehicle decreased 16.9% with increasing the track ground contact length from 1.30 to 2.0m when the track width is kept constant at 0.3m. From the justification of vehicle motion resistance based on vehicle track width and length, the vehicle track width 0.3m and length 2.0m could be considered for the track system of the vehicle in order to get the vehicle ground contact pressure of 16.35kN/m^2 and to avoid excessive motion resistance. Therefore, it was found that for a given overall dimension of 0.3mx2.0m track system, the motion resistance coefficient of the 19.62kN vehicle is 12%, which could be good enough for a track vehicle on soft terrain [9].

Based on Figures 12 to 14, it could be pointed out that if the 19.62kN vehicle track size is considered to be 2.0X0.3m^2, the ground pressure exit on track-terrain interfaces is 16.35kN/m^2 with sinkage of 0.09m and motion resistance coefficient of 12%. Therefore, the 19.62kN vehicle track system overall dimension can be optimised by selecting track width of 0.3m and ground contact length of 2.0m.

4.2 Track Grouser Size

To fully utilize the shear strength of the peat surface mat for generating tractive effort, the use of grouser on tracks would be required. From the field experiment on Sepang, it was found that the shear strength of the peat surface mat is considerably higher than that of the underlying peat deposit and that there is well defined shear-off point beyond which the resistance to shearing is significantly reduced. This would, however, considerably increase the risk of tearing off the surface mat unless the slip of the track is properly controlled. Thus, the use of aggressive grouser on vehicles for use in organic terrain does not appear to be desirable from traction as well as environmental viewpoints. The surface mat thickness of Sepang peat terrain was found to be about 0.1m. In order to fully utilize the shear strength of the surface mat and to increase the trafficability of the terrain the grouser height of the track is considered to be 0.06m.

4.3 Sprocket location and Size

The location of drive sprocket has a noticeable effect on the vehicle tractive performance. Wong et. al. [14] reported that in forward motion, the top run of the track is subjected to higher tension when the sprocket is located at the front than when the sprocket is located at the rear. Thus, with a front sprocket drive, a larger proportion of the track is subjected to higher tension and the overall elongation and internal losses of the track will be higher than with a rear sprocket drive. With higher elongation, more track length is available for deflection and the track segments between road-wheels take fewer loads and the vibration of the track increase, which will cause the fluctuation of the track. Consequently, the sinkage and motion resistance will be higher and the mobility of the vehicle will be affected severely on the unprepared peat terrain. Therefore, the sprocket could be considered to be located at the rear part of the track system configuration in order to distribute the vehicle normal pressure to the track-terrain interfaces more uniformly. The center point of the sprocket is considered the (0,0) coordinate system of the vehicle.

From the simulation results, it was found that the ratio of the sprocket diameter to track pitch have significant effect on the vehicle tractive performance. Therefore, sprocket diameter to track pitch should be a value which will stand to meet the field requirement. Figure 15 shows the variation of the torque of the sprocket and the tractive efficiency with the ratio of the sprocket diameter to track pitch. The vehicle under consideration is total weight of 19.62kN including payload 9.81kN and is traversing on a zero slope terrain with speed fluctuation of

2.75% at travel speed of 10km/hr. Therefore, the diameter of the sprocket can be computed using the following equation of Wong et. al. [12]:

$$\delta = 1 - \sqrt{\left[1 - \left(\frac{T_p}{D_{rs}}\right)^2\right]} \tag{15}$$

where δ is the speed fluctuation, T_p is the track pitch and D_{rs} is the diameter of the sprocket. If the vehicle speed fluctuation of 2.75% and track pitch of 0.1m for the track system configuration are taken into account, the computed value of the sprocket diameter for the vehicle track system is 0.43m. It is shown that the ratio of sprocket diameter to track pitch of 4.3 track system vehicle able to develop the torque of 4850N-m and tractive efficiency of 73.5%, which is good enough for an off-road vehicle on peat or soft terrain. This conclusion is further supported by the relationship between the turning radius and turning performance. Figure 16 shows that torque of the sprocket decreases and turning moment increases with increasing vehicle turning radius. For a given turning radius of 2m, the vehicles sprocket torque development should be in the ranged of 3200 to 4300N-m and 3800 to 6200N-m at turning speeds of 6 and 10km/hr, respectively in order to overcome the turning moment resistance of 2800N-m and 3800N-m, respectively. Therefore, the diameter of the sprocket for the vehicle track system can be optimized to 0.43m in order to develop sufficient torque for overcoming the turning moment.

4.4 Idler location and size

Idler is located at –2.0m front of the sprocket of track system as shown in Figure 8. The vehicle sinkage for the Sepang peat terrain should not be considered more than or equals to 0.1m since the surface mat thickness of peat is 0.1m as earlier reported. Therefore, from the relationship between the vehicle sinkage, track entry angle and idler diameter, the idler diameter can be identified. Figure 17 shows that the vehicle track entry angle at front idler and sinkage decreases with increasing vehicle front idler diameter. For a given vehicle sinkage of 0.09m, the vehicle front idler could be considered 0.4m and the corresponding track entry angle of 75°. This conclusion can be further supported from the relationship between the track entry angle, slippage and vehicle tractive performance. Figure 18 shows that the relationship between the vehicle track entry angle, slippage, and tractive efficiency. At track entry angle 75°, the vehicle slippage and tractive efficiency were found 21% and 73.67%, respectively, which was found at sprocket size of 0.43m. Therefore, the front idler diameter 0.4m can be considered for the track system of the vehicle.

4.5 Road-wheel diameter, Track pitch, and Number of road-wheel

Wong et al. [12] reported that the ratio of road wheel spacing to track pitch is a significant parameter that affects the tractive performance of tracked vehicle, particularly on soft terrain. The decrease in the track motion resistance coefficient with the increase of the number of road wheels was primarily due to the reduction in the peak pressures and sinkage under the road wheels. The longer track pitch would lead to an improvement in tractive performance over soft terrain. It may cause a wider fluctuation in vehicle speed and higher associated vibration. Consequently, a proper compromise between tractive performance and smoothness of operation must be struck.

Road-wheel diameter can be predicted based on the following equation:

$$S_r = \frac{D_1}{2} + \frac{D_2}{2} + G \tag{16}$$

where, S_r is the road-wheel spacing, D_1 is the first road-wheel diameter, D_2 is the second road-wheel diameter and G is the gap between consecutive road-wheel is assumed to be 5mm for avoiding the track deflection between the consecutive road-wheel. In the track system all the road-wheel dimension are considered as equal size.

Figure19 shows that the vehicle drawbar pull increases with increasing ratio road-wheel spacing to track pitch and tractive efficiency increases with increasing the ratio of road-wheel spacing to track pitch until 2.1 and then decreases with further increasing of the ratio of road-wheel spacing to track pitch. If the ratio of road-wheel spacing to track pitch is considered to be 2.45, the tractive efficiency of the vehicle is found 73%. Whereas, the tractive efficiency of the vehicle is found 73% for the optimum size of sprocket diameter of 0.43m and idler diameters of 0.4m. Therefore, the road-wheel spacing to track pitch should be 2.45 if the optimum sprocket and idler diameters are limited to 0.43m and 0.40m, respectively. By using S_r/T_p equals to 2.45 and S_r equals to 24.5cm, the computed value of T_p equals to 10cm.

The number of road-wheels can be computed based on the following equation based on Figure 2:

$$L - \frac{D_{rs}}{2} - \frac{D_{fi}}{2} - G = \left(D_r + G\right) n_r \tag{17}$$

where, L is the total ground contact length in cm, D_{rs} ,D_{fi} and D_r are the diameter of the sprocket, front idler and road-wheel, respectively and n_r is the number of road-wheel.

By using L equals to 2.0m, D_{rs} equals to 0.43m, D_{fi} equals to 0.40m, D_r equals to 0.22m, G equals to 5mm, the computed value of n_r is 7. Therefore, total number of road-wheel seven with diameter of 0.24m on the 19.62kN vehicle track system would significantly reduce vehicle vibration during traversing on the unprepared peat terrain by making approximate zero deflection of the track between two consecutive road-wheel.

4.6 Center of Gravity Location

Center of gravity of a tracked vehicle is a most important design parameter for getting the high tractive performance. Figure 20 shows, the vehicle of total weight 19.62kN including payload 9.81kN is traversing on a zero slope terrain with traveling speed of 10km/hr, the maximum tractive efficiency with center of gravity located at 0.30m ahead the mid-point of the track ground contact length are 10% higher than the vehicle center of gravity located at the mid-point of the track ground contact length. This may be happened due to the variation of external motion resistance exerted for the track different sinkaging value between front part and rear part. Therefore, the location of vehicle center of gravity can be optimized at 0.3m ahead of mid point of the ground contact track of the vehicle.

The basic design parameters of the vehicle found from the simulation study are shown in Table 2.

5.0 VEHICLE DESIGN

Conventional amphibious segmented metal molded rubber track vehicles are based on custom built, hydrostatic skid-steer transmission systems. To turn, the track on one side of the unit is stopped while the other side is left to do all of the work. The designing of the vehicle with a moderate weight upto 19.62kN including 9.81kN payload and a high ground contact area will provide the vehicle lower normal ground pressure of 12kN/m^2 which will allow the vehicle lower sinkage and rolling resistance thus will provide the high tractive effort, yielding higher travel speeds and vehicle productivity on the super weak peat terrain. Steering of this machine is by means of two levers to control the movement forward, backward, 'stop', left or right. The vehicle can power both sides of the unit independently. This results in a much smoother ride, and increased maneuverability and responsiveness. Geometrical arrangement of the vehicles engine, gearbox, hydraulic pumps, hydraulic tank, fuel tank and hydraulic motor and undercarriage components on the vehicle frame resulting in equal and balance loading which reduce any uneven problems during operations on unprepared peat terrain both in straight and turning motion. For the operator this means a less responsive for eliminating dangerous shuffling of load to ride the vehicle on the peat terrain even in tight spot.

Computer Aided Design (3D-CAD) software package was used to develop the three-dimensional design of the machine components. All of the components of the vehicle such as vehicle structural frame, gear boxes, undercarriage including track, front idler, road-wheel, rear sprocket, supporting wheel and tension device, hydraulic tank and fuel tank have been designed based on the optimized design parameter as shown in Table 3 and the isometric view of the proposed vehicle has shown in Figure 21.

6.0 CONCLUSION

(i) The presenting materials of this paper may provide an integrated idea in case of designing an off-road rubber tracked vehicle on low bearing capacity peat terrain.

(ii) Most of the algorithm presented can be considered for the parametric study of wheel vehicle on peat terrain.

(iii) Based on the simulation result, it was found that 2.0x0.3m^2 tracked ground contact area may ensure the 19.62kN vehicle to traverse on peat terrain without making any serious problem.

(iv) Based on the simulation result, it was found that the maximum tractive efficiency of 19.62kN vehicle with center of gravity located at 0.30m ahead the mid-point of the track ground contact length is 10% higher than the vehicle center of gravity located at the mid-point of the track ground contact length.

AKNOWLEDGEMENT

This research project is classified under RM7 IRPA Project No. 01-02-04-0135. The authors are very grateful to the Ministry of Science, Technology and The Environment of Malaysia for granting the financial assistance.

NOTATIONS

θ_{fi}	Track entry angle at front idler,°
θ_{ti}	Track trim angle,°
θ_{rs}	Track exit angle at rear sprocket,°
φ	Peat internal frictional angle, °
α	Grouser setting angle with track, °
β_{rr}	Roadwheel rotational angle for max. shear strength, °
τ	Peat terrain shearing stress, kN/m^2
σ	Vehicle normal stress, kN/m^2
γ_d	Peat bulk density (dry basis), kN/m^3
ω	Moisture content,%
δ	Track fluctuation, %
B	Track width,m
C	Peat terrain coghesiveness, kN/m^2
$C.G$	Vehicle centre of gravity
D_{hfi}	Peat terrain hydraulic diameter due to front idler,m
D_{hmp}	Peat terrain hydraulic diameter due to main partl,m
D_{hrs}	Peat terrain hydraulic diameter due to rear sprocket,m
D_p	Drawbar pull, kN

D_r	Roadwheel diameter,m
D_{rs}	Rear sprocket diameter,m
E	Distance of the track midle point to C.G,m
e^1	Exponential
F_b	Vehicle tractive effort at track bottom part,kN
F_{fib}	Vehicle tractive effort at idler bottom track part,kN
F_{rsb}	Vehicle tractive effort at sproket bottom track part,kN
F_{mb}	Vehicle tractive effort at main part bottom track part,kN
F_s	Vehicle tractive effort at track side,kN
F_{fis}	Vehicle tractive effort at idler track side,kN
F_{rss}	Vehicle tractive effort at sprocket track side,kN
F_{ms}	Vehicle tractive effort at main track track side,kN
F_{tt}	Total tractive effort,kN
H	Grouser height, m
h_{cg}	C.G height,m
I	Vehicle slippage, %
i_{fi}	Slippage of the front idler,%
i_{rs}	Slippage of the rear sprocket,%
i_{mp}	Slippage of the track main part ,%
j_x	Shear dispalcement for track small part,m
K_w	Shear deformation modulus,m
K_{wfi}	Shear deformation modulus for front idler,m
K_{wrs}	Shear deformation modulus for rear sprocket,m
K_{wmp}	Shear deformation modulus for track main part,m
k_p	Underlying peat stiffness, kN/m^3
L	Length of the track ground main part,m
L_{fib}	Length of the front idler bottom track part,m
L_{rsb}	Length of the rear sprocket bottom track part,m
m	Peat surface mat stiffness, kN/m^3
n	Number of road-wheel
P_0	Reaction force at the track main part, kN/m^2
P_{fi}	Reaction force at the idler track part, kN/m^2
P_{rs}	Reaction force at the sprocket track part, kN/m^2
Q	Torque of the sprockt, kN-m
R_{fi}	Front idler radius,m
R_{rs}	Rear sprocket radius,m
S_r	Spacing between consecutive roadwheel,m
T	Initial track tension, kN
T_p	Track pitch, m
V_t	Vehicle theoritical speed, km/hr
W	Vehicle total weight including 0.981kN, kN
x	Track divisional distance,m
z_c	Vehicle critical sinkage,m

z_{fi} Sinkage of the front idler,m
z_{rs} Sinkage of the rear sprocket,m
z_{mp} Sinkage of the track main part,m
z_n Sinkage of the n number road-wheel, m

REFERENCE

1. Hitam, A and Zamri, A., "Tracked vehicle for fresh fruit bunches infield collection", *Proceedings Agricultural Conference, PORIM International Palm Oil Congress*, 277-279, 1996.
2. Ooi, H.S. Design and development of peat prototype track type tracktor. MARDI report no.184, 1996.
3. Yahya, A., Jaafar, M.S., and Aribi, K., "Mechanical infield collection of oil palm fresh fruit bunches", *Fruit, Nut, and vegetable production engineering*. Vol.1, 317-326, 1997.
4. KUBOTA KC-50L. http://www.tracksandwheel/kc50L.htm).
5. Hitachi EG30- Rubber Crawler Carrier. http://www.hcmac.com/products/pr_sw/eg30.html
6. SEIREI- SC3.SC3W and SEIREI - 600D. Sales Brochure,SEIREI Industry Co.Ltd, 2002
7. Wong, J. Y., Radforth, R., and Preston-Thomas, J,. "Some futher studies on the mechanical properties of muskeg in relation to vehicle mobility",. *Journal of Terramechanics*. 19(2): 107-127, 1982.
8. Wong, J. Y., Garbber, M., Radforth, J. R. and Dowell, J. T., "Characterization of the mechanical properties of muskeg with special reference to vehicle mobility",. *Journal of Terramechanics* 16(4),163-180, 1979.
9. Wong, J.Y., "Optimization of design parameters of rigid-link track systems using an advanced computer aided method", *Proc. Instn. Mech. Engrs*, 208(D), 153-167, 1998.
10. Ataur, R., Azmi, Y., Zohadie, M., Desa, A., Wan, I., and Kheiralla, A., "Mechanical Properties in Relation to Vehicle mobility of Sepang Peat Terrain in Malaysia", *Journal of Terramecanics*: 41(1), 24-45, 2004.
11. Bekker, M.G., *"Theory of land locomotion"*, (The Mechanics of Vehicle Mobility). Ann Arbor: University of Michigan Press: 233-275, 1969.
12. Wong, J. Y., *"Theory of Ground Vehicle"*, Second Edition, John Wiley & Sons Inc. New York: 2001.
13. Ooi, H.S., Performance of Modified Kubota Carrier RC20P and Porter P6-121 on peat soil. MARDI Report no.110, 1986.
14. Wong, J.Y., *"Terramechanics Off-Road Vehicles"*, Elsevier Science Publisher, Amsterdam, Netherland, 1989.

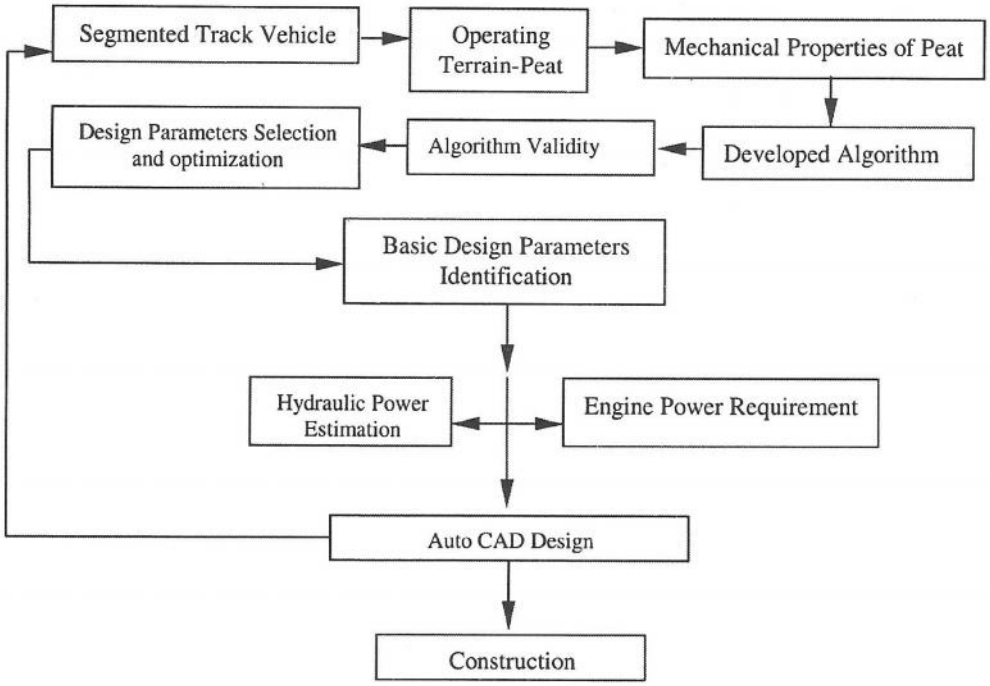

Figure 1 Flow chart for designing framework a segmented tracked vehicle

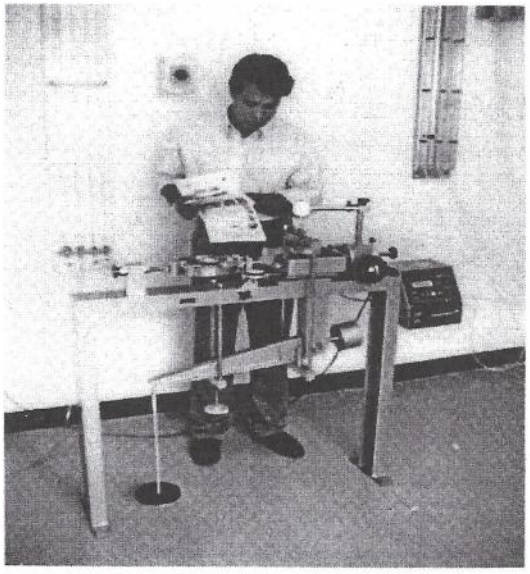

Figure 2 Wykeham Farrance 25402 shear box apparatus

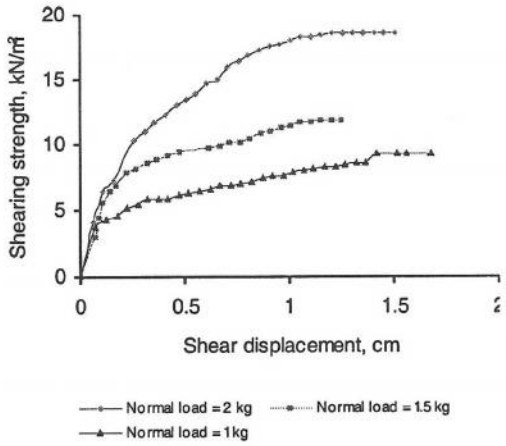

Figure 3 Typical trend of shearing strength versus shear displacement

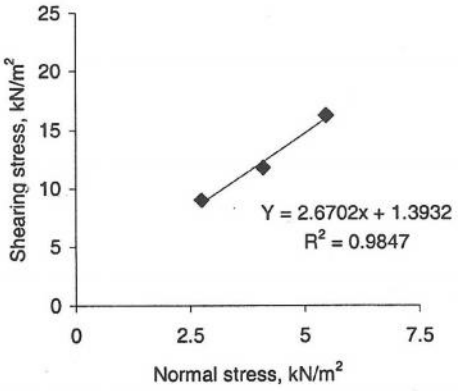

Figure 4 Typical trend of shearing strength versus normal stress

Figure 5 RMU I012 digital vane shear test apparatus

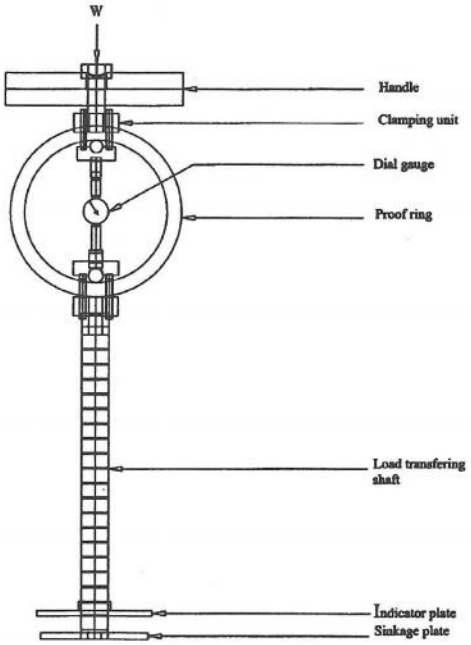

Figure 6 Bearing capacity measuring apparatus

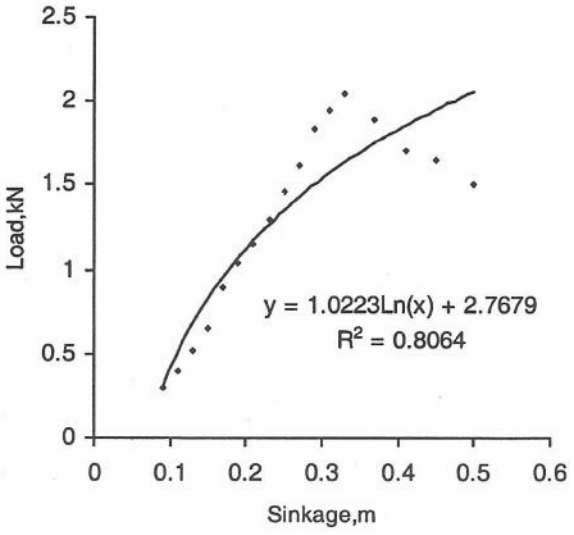

Figure 7 Typical load-sinkage trend of peat

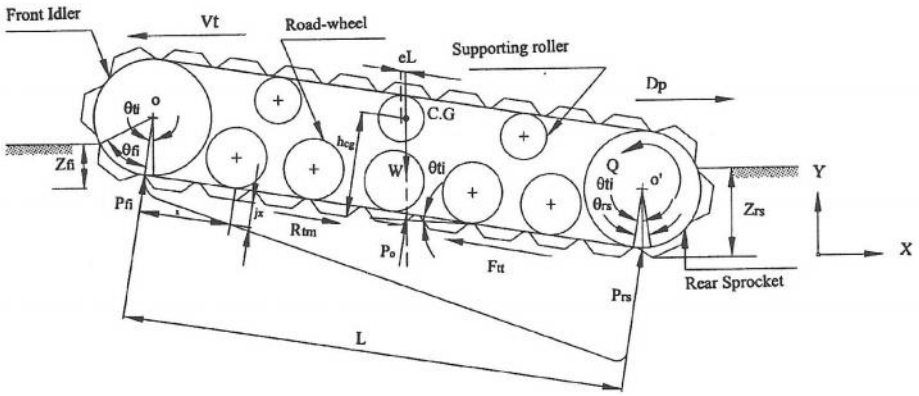

Figure 8 Force acting on the track system of the vehicle during traversing on peat terrain with slippage 10%

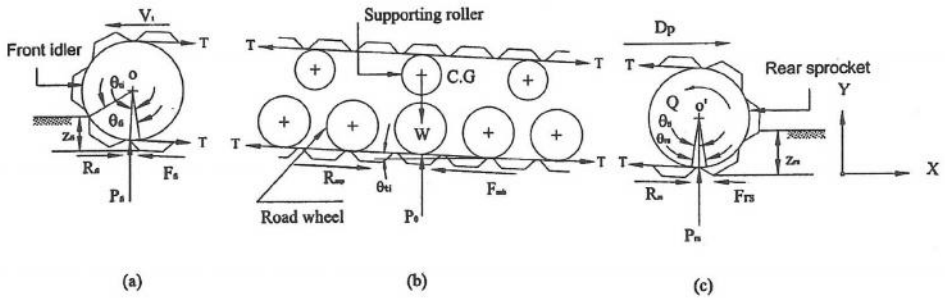

Figure 9 Force diagram on the track system segmented components (a) Front idler, (b) Track main straight part, and (c) Rear sprocket

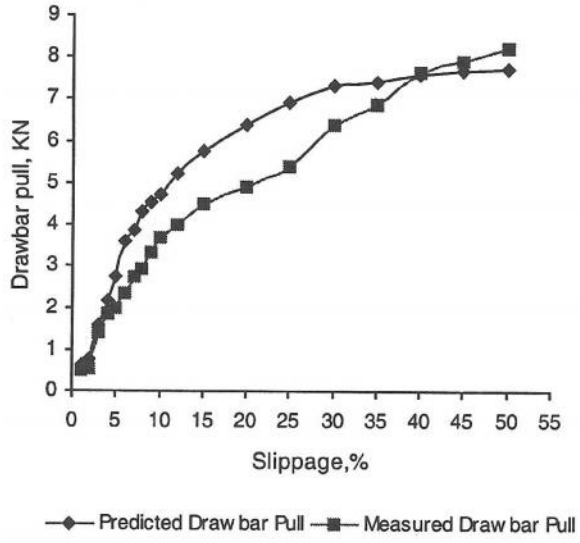

Figure 10 Variation drawbar pull with slippage

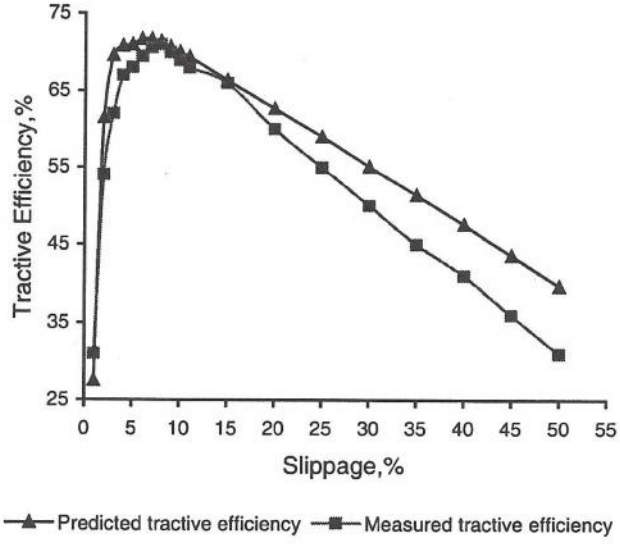

Figure 11 Variation of Tractive efficiency with slippage

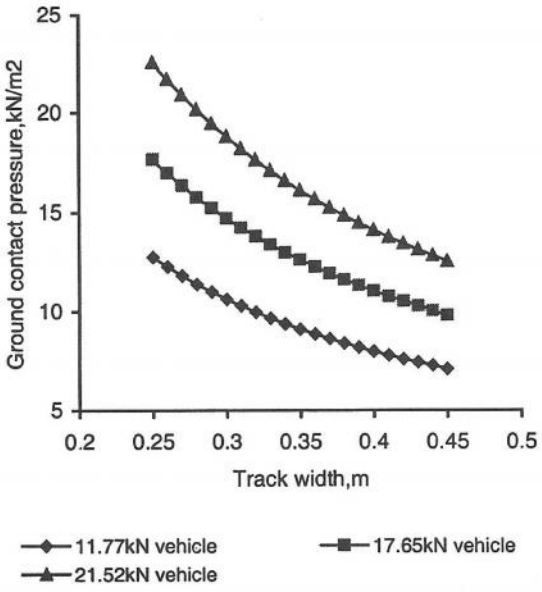

(a)

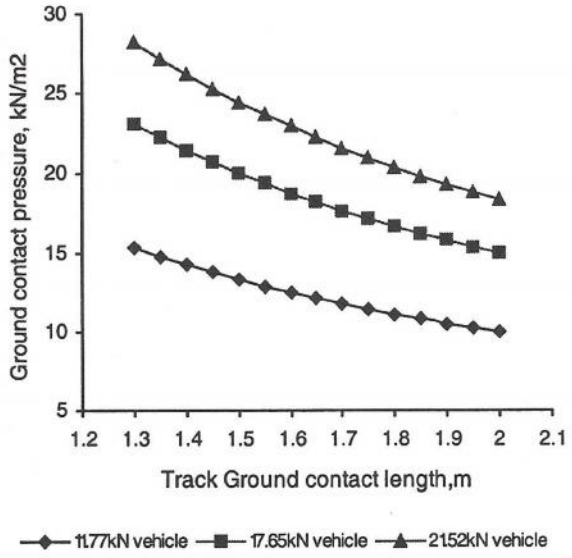

(b)

Figure 12 Variation of ground pressure distribution with (a) variation of track width at constant track ground contact length of 200cm and (b) variation of track ground contact length at constant track width of 30cm

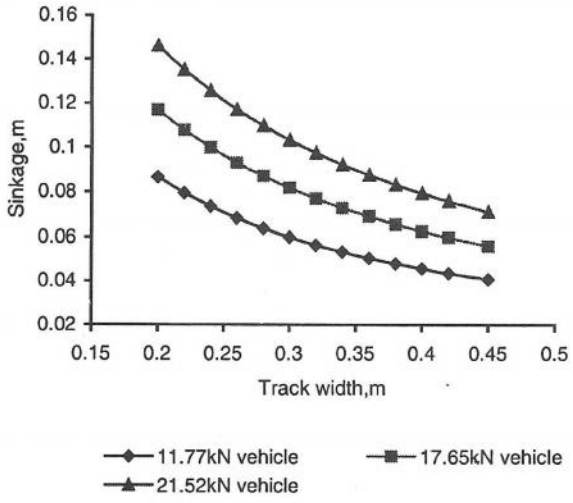

(a)

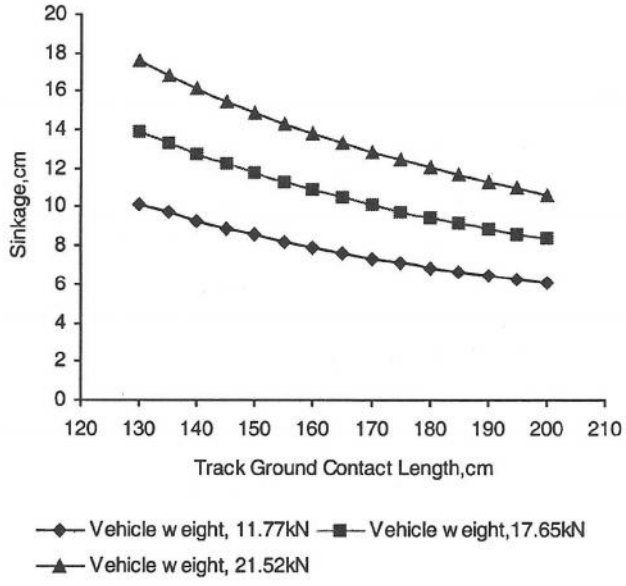

(b)

Figure 13 Variation of vehicle sinkage with (a) variation of track width at constant track ground contact length of 200cm and (b) variation of track ground contact length at constant track width of 30cm.

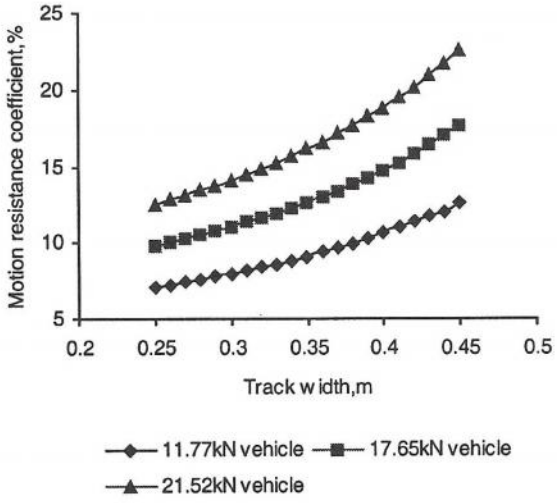

(a)

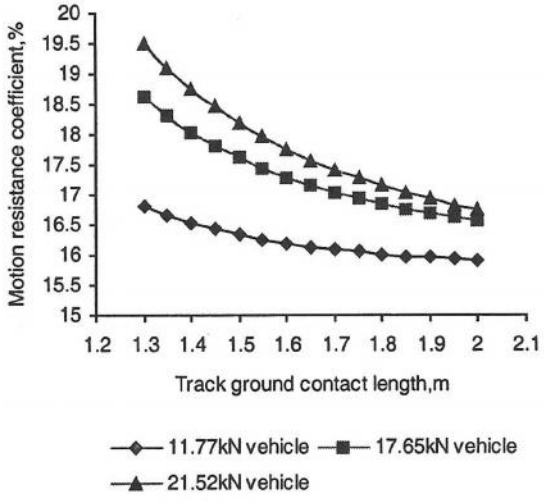

(b)

Figure 14 Effect of track size on vehicle tractive performance (a) track width and (b) track ground contact length

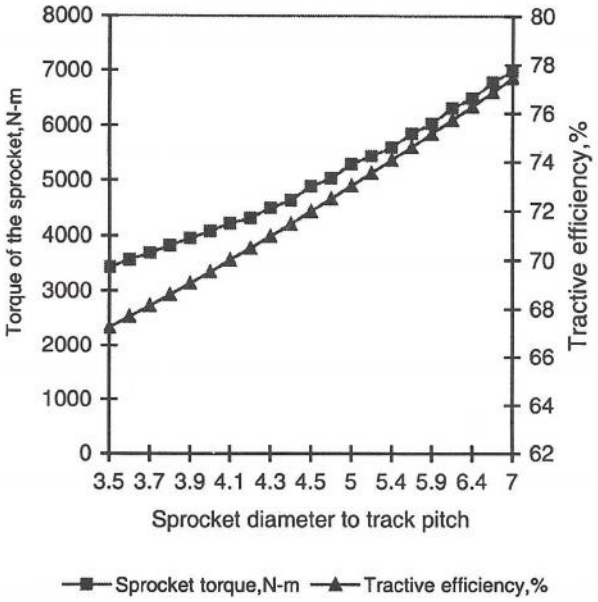

Figure 15 Variation of tractive efficiency and sprocket torque with sprocket diameter

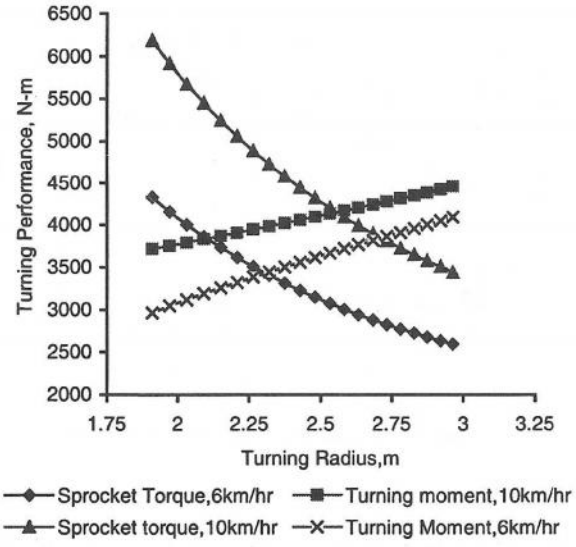

Figure 16 Variation of sprocket torque and turning moment with turning radius

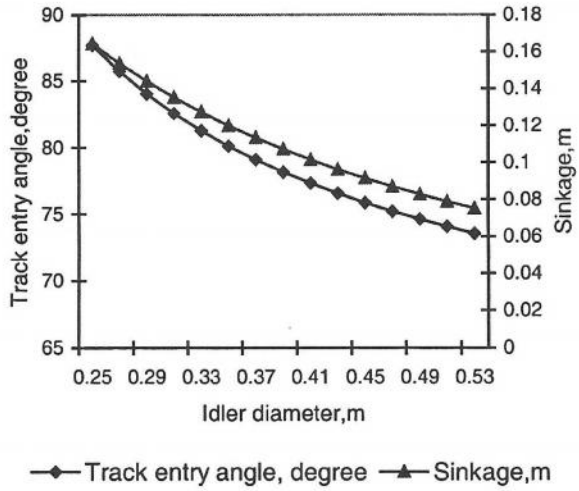

Figure 17 Relationship between track entry angle, sinkage and idler diameter

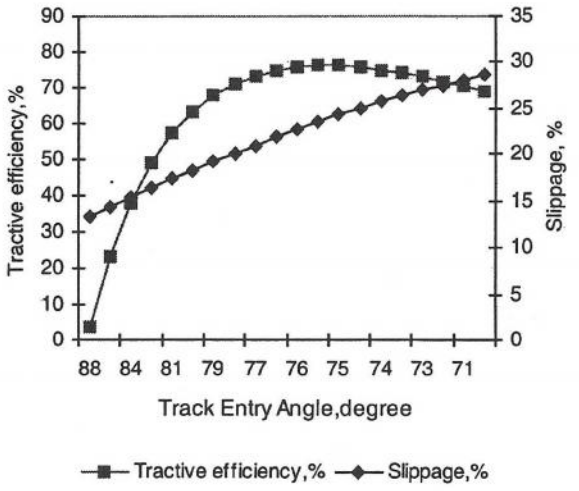

Figure 18 Track entry angle, tractive performance and slippage

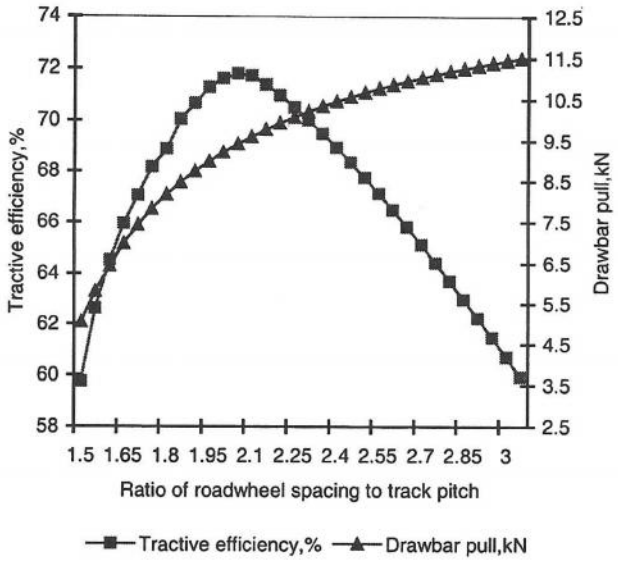

Figure 19 Relationship between tractive efficiency, drawbar pull and the ratio of the road-wheel spacing to track pitch

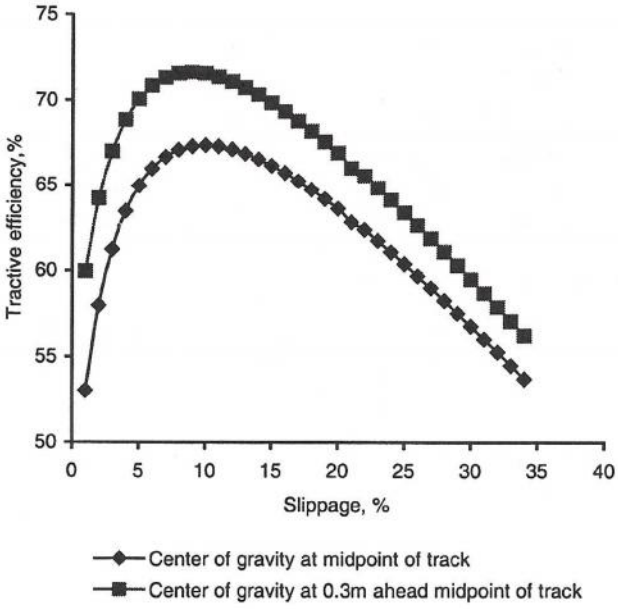

Figure 20 Relationship between tractive efficiency and slippage

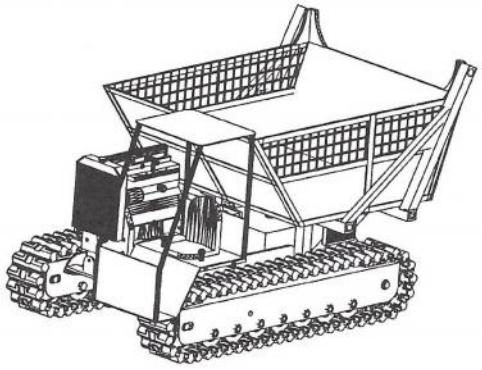

(a)

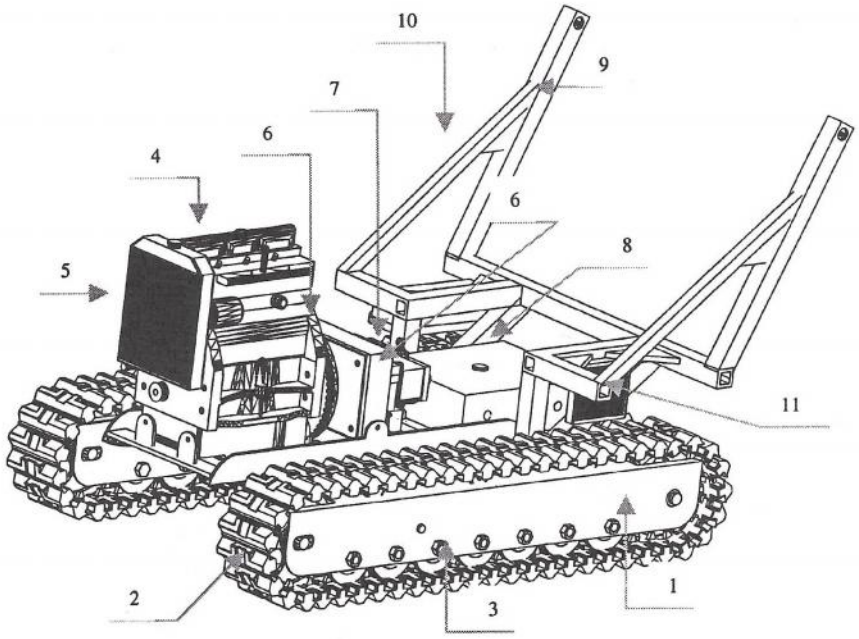

1.Track Frame	5. Radiator	9.Hydralic tank
2. Segmented Rubber Trcak	6.Gear box	10. Fork arm
3.Road-wheel	7.Pump	10. Renforcement
4.Engine	8. Telescopic cylinder	11. Heat Exchaner

Figure 21 Isometric view of the full vehicle. (a) with container, (b) without container and full vehicles (c) front view and (d) side view

Table 1 Sepang peat terrain parameters

Parameters	Un-drained		Drained	
	Mean value	SD	Mean value	SD
ω, (%)	83.51	-	79.58	-
γ_d, (kN/m^3)	1.53	0.59	1.82	0.78
c, kN/m^2)	1.36	0.21	2.73	0.39
φ, (degree)	23.78	4.56	27.22	2.19
K_w, (cm)	1.19	0.10	1.12	0.17
m_m,(kN/m^3)	27.07	13.47	41.79	13.37
k_p, (kN/m^3)	224.38	52.84	356.8	74.27

Notification: SD-Standard deviation

Source: Ataur et.al (2004).

Table 2 Basic parameters of Kubota Carrier RC20P track vehicle

Parameters	Values
Vehicle parameters	
Machine weight, kN	1645
Max. loading capacity, kN	1000
Rated power, kW@rpm	8.2@3200
Track parameters	
Ground contact length,m	1.85
Width,m	0.43
Grouser height,m	0.05
Machine parameters	
Length,m	2.98
Width,m	1.76
Height,m	1.45
Ground clearance,m	0.27

Source: MARDI REPORT NO.110

Table 3 Basic design parameters of the special segmented rubber tracked vehicle

Vehicle Parameters	
Total weight including 9.81kN payload, kN	19.62
Vehicle traveling speed, km/hr	10
Center of gravity, x coordinate, m	-0.80
Centre of gravity, y coordinate,m	0.45
Sprocket radius , m	0.215
Idler radius, m	0.20
Idler center, x coordinate, m	-2.0
Idler center, y coordinate, m	0
Number of road-wheels (each side)	7
Road-wheel radius, m	0.12
Road-wheel spacing, m	0.245
Number of supporting rollers (each side)	3
Supporting rollers radius, m	0.10
Track Parameters	
Track total length (each side), m	5.90
Track pitch, m	0.10
Track width, m	0.30
Track ground contact length, m	2.00
Road-wheel spacing to track pitch	2.45
Vehicle speed fluctuation, percentage	5
Grouser height, m	60

Note: Coordinates origin is at the center of the sprocket. Positive x and y coordinates are to the rear and top, respectively.